

Indium Thiosemicarbazones

Trigonal-Bipyramidal vs. Octahedral Coordination in Indium(III) Complexes with Potentially *S,N,S*-Tridentate Thiosemicarbazones

Federico Salsi,^[a] Maximilian Roca Jungfer,^[a] Adelheid Hagenbach,^[a] and Ulrich Abram*^[a]

Abstract: Three bis-chelates of indium(III) with (partially fluorinated) *S,N,S*-tridentate thiosemicarbazones (H_2L) were prepared and their structures were studied in solution and in the solid state by NMR, ESI MS and single-crystal X-ray diffraction. The three compounds are isostructural in solution with five-coordinate In^{III} ions and two differently coordinated thiosemicarbazonato ligands, $[In(L)(HL)]$. A temperature-dependent 1H NMR study reflects the presence of dynamic processes in the

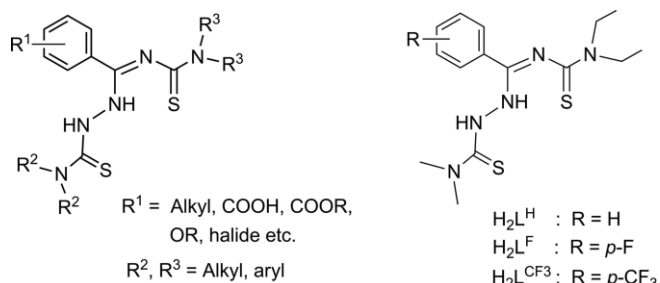
molecules such as the resolution of hindered rotation around CN bonds with partial double-bond character and the pH-triggered isomerization between 5- and 6-coordinate species. The latter is confirmed by the isolation of compounds with different solid-state structures, $[In(L)(HL)]$ and $[In(L)_2]^-$, depending on fluorine-substitutions in the periphery of the thiosemicarbazones.

Introduction

Main medical applications of In^{III} complexes are currently related to the use of the isotope ^{111}In (electron capture with gamma emissions of 171 and 245 keV, $t_{1/2} = 67.4$ h) in diagnostic radiopharmacy,^[1–4] where it is frequently used for the imaging of infection and inflammation sites. Additionally, ^{111}In is under discussion for cancer therapy, since it also emits Auger electrons, offering a method to achieve DNA damage and eventual cell death.^[5] Non-radioactive indium(III) compounds also present a number of pharmacological applications. Complexes with phthalocyanines are under study as photo-sensitizers in photodynamic therapy for cancer treatment and other indium(III) complexes have also been proven to exhibit antimicrobial and antiproliferative activities.^[6–11]

The development of metal-based radiopharmaceuticals requires a thorough knowledge of the coordination chemistry of the metal, in order to optimize the ligand design. Like for the related medically relevant metal gallium, the only stable aqueous oxidation state of indium is +3. In this oxidation state, indium is a hard Lewis acid with high affinity for water. Hence, hydrolysis of indium complexes in the biological medium is a primary concern in practical applications. The coordination chemistry of indium is, in many cases, unpredictable because of its high diversity. Indium complexes present coordination numbers from 3 to 8 with a large variety of geometries. For

applications in radiomedicine, a high stability and/or inertness of the complexes is required. In order to avoid hydrolysis and afford sufficient stability in the biological medium, polydentate ligands are commonly used. Despite its importance, the coordination chemistry of indium with multidentate ligands is still a mostly unexplored field.^[12,13] Frequently used chelators in radiomedicine are polyamino acids, e.g. EDTA, DTPA, DOTA, TACN. Their high coordination numbers (6–8) and the hard character of the donor sites affords stabilisation through electrostatic and unspecific ligand-ion interactions.^[14] On the other hand, indium is also capable to form stable adducts with softer bases or bases with intermediate character (P, S, Cl, Br, I), which might allow the formation of bonds with a higher degree of covalence and specificity. An interesting and versatile class of ligands with soft sulfur donor atoms are thiosemicarbazones, but there are only a few examples of related indium complexes.^[15–21] Some systematic studies with thiosemicarbazonato chelates of indium(III) with regard to medical applications have recently been done by H. Beraldo et al.^[22–24] The promising results of these investigations stimulated us to undertake some experiments with potentially *S,N,S*-tridentate thiosemicarbazone ligands derived from *N,N*-dialkyl-*N'*-benzoylthioureas (see Scheme 1).

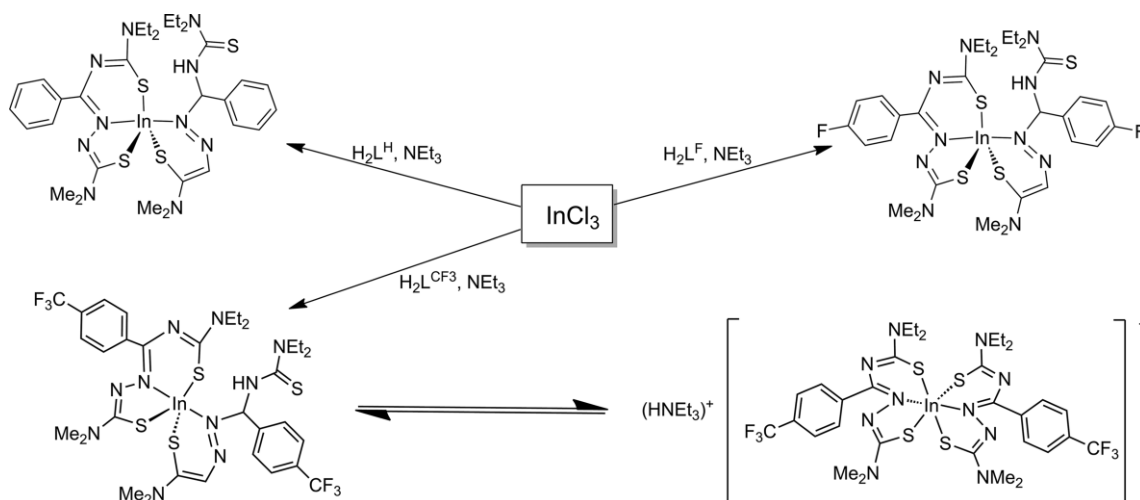


Scheme 1. Structural versatility of potentially tridentate *S,N,S*-thiosemicarbazone ligands derived from *N,N*-dialkyl-*N'*-benzoylthioureas and specification of the compounds used in the present work: H_2L^H , H_2L^F , $H_2L^{CF_3}$.

[a] U. Abram, Freie Universität Berlin, Institute of Chemistry and Biochemistry, Fabeckstr. 34-36, 14195 Berlin, Germany
E-mail: ulrich.abram@fu-berlin.de
<https://www.bcp.fu-berlin.de/chemie/chemie/forschung/InorgChem/agabram/index.html>

Supporting information and ORCID(s) from the author(s) for this article are available on the WWW under <https://doi.org/10.1002/ejic.201901356>.

© 2020 The Authors. Published by Wiley-VCH Verlag GmbH & Co. KGaA. This is an open access article under the terms of the Creative Commons Attribution License, which permits use, distribution and reproduction in any medium, provided the original work is properly cited.



Scheme 2. Synthesis of the In^{III} complexes with *S,N,S*-tridentate thiosemicarbazones.

Such compounds are very versatile chelators with intermediate hard-soft properties. They can deprotonate once or twice affording very flexible charge compensation of the metal ion. Besides, the high degree of electronic delocalisation in the ligand affords an efficient distribution of the negative charge all over the system, yielding stability.^[25] The organic residues can easily be functionalized and some of their metal complexes show promising anti-parasitic activity.^[26–29]

For the present structural study on related indium complexes, we used three ligands with different substituents on the phenyl ring: H_2L^H , H_2L^F and $H_2L^{CF_3}$ (for formulae see Scheme 1).

Results and Discussion

The addition of two equivalents of the thiosemicarbazone H_2L^H to a solution of $InCl_3$ in methanol gives an insoluble colorless solid, which is probably a less-defined, polymeric compound, which resisted any structural characterization. The addition of a supporting base such as NEt_3 together with H_2L^H or directly thereafter results in the re-dissolution of the intermediately formed solid and the formation of a yellow solution, from which a light-yellow precipitate deposits within a few seconds (Scheme 2). Solutions of the resulting solid in $CHCl_3$ are unstable at room temperature and slowly decompose with formation of a white insoluble material. Such a behavior has been observed before for the non-coordinated, fluorine-substituted ligands.^[26] A considerable stabilization could be achieved by the complexation on rhenium(V) or gold(III) centers,^[27–29] but not with In^{III} . However, solutions of the In^{III} complexes are stable at 0 °C to perform all necessary chemical manipulations and at –20 °C for an indefinite time. The 1H NMR spectrum of the compound at room temperature in chloroform confirms that the thiosemicarbazone is coordinated to the metal. All signals are shifted and change their multiplicity in comparison to the uncoordinated ligand. A more careful analysis shows the presence of two coordinated, non-equivalent ligands in a 1:1 ratio. This becomes obvious by the presence of two singlets related to the NMe_2 groups of the ligand at about 3 ppm. The asymmetry of the complex is also reflected in the region of the aromatic pro-

tons by an increase of the complexity of the signals. A signal at 9.25 ppm can be assigned to a single NH proton. This is consistent with the formation of a bis-chelate, in which one ligand molecule is dianionic (both NH deprotonated) and the other one is monoanionic (only one NH deprotonated): $[In(L^H)(HL^H)]$. The resulting neutral In^{III} complex should be poorly soluble in MeOH, which explains its precipitation from the methanolic reaction mixture. Moreover, no signals of a potential (organic) counterion can be detected in the 1H NMR spectrum of the product.

The aliphatic region of the 1H NMR spectrum of $[In(L^H)(HL^H)]$ shows four broad signals in the range between 3.3 and 4.0 ppm for the CH_2 protons of the diethyl amino groups. The non-equivalence of the protons in the ethyl chain is due to a hindered rotation around the C–N bond, which has a partial double bond character. This is frequently observed for complexes with this class of ligands.^[25] Each non-equivalent ligand generates two multiplets, corresponding to the two methylene groups. The signals at highest field are the CH_3 of the diethyl amino groups, which consist in two overlapping peaks with integral ratio 1:1. One is a well-defined triplet, the other one is a broad signal with undefined multiplicity. The broadening indicates that the methyl groups of one of the two chelating ligands are involved in a dynamic process. The measurement of temperature-dependent 1H NMR spectra confirmed this assumption. The temperature was varied from +20° to –30° C in intervals of 10 degrees (see Figure 1 and Supporting Information). At –20° C the broadened signals split into the corresponding resolved multiplets. The region between 1.13 and 1.40 ppm shows a set of six triplets corresponding to six methyl groups of the ethyl chains. Between 3.24 and 4.05 ppm appear eight multiplets corresponding to the eight non-equivalent protons belonging to the same ethyl group. As a consequence of the partial double bond character of C– NEt_2 bonds, the methylene groups cannot rotate; each proton has a different chemical shift and couples with the adjacent methyl protons and with the geminal proton. The CH_3 groups can rotate, but they are blocked in fixed positions, so each of them has a different environment and gives a triplet with different chemical shift. Solu-

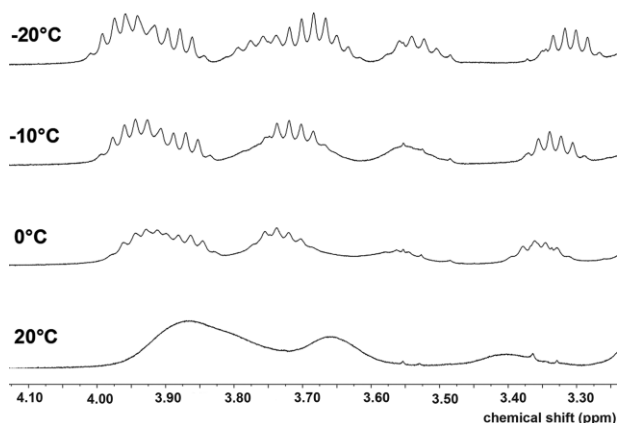


Figure 1. Temperature dependence of the ^1H NMR signals belonging to the methylene groups.

tions of $[\text{In}(\text{L}^{\text{H}})(\text{HL}^{\text{H}})]$ are not stable enough to record ^{13}C NMR spectra of sufficient quality.

Elemental analysis confirms the purity of the obtained product. The most intense signal in the ESI+ MS spectrum of $[\text{In}(\text{L}^{\text{H}})(\text{HL}^{\text{H}})]$ is the peak of the protonated molecular ion. Also adducts with Na^+ and K^+ ions and some fragmentation products could be identified.

The IR spectrum of the solid shows the presence of the NH stretch of the thiosemicarbazone at 3238 cm^{-1} and an intensive band at 1493 cm^{-1} , which can be assigned to the C=N stretch.

Single crystals of $[\text{In}(\text{L}^{\text{H}})(\text{HL}^{\text{H}})]$ were obtained from a saturated solution of the complex in benzene. An X-ray structure determination confirms the results of the spectroscopic studies, that the product is a neutral compound with two differently bonded thiosemicarbazonato ligands (Figure 2). One of the ligands is doubly deprotonated and binds to the metal tridentate via its S,N,S donor atom set, while the second ligand establishes only one five-membered chelate ring via the nitrogen and sulfur atoms of the thiosemicarbazone moiety. The sulfur atom of the thiourea unit remains uncoordinated and the adjacent nitrogen atom remains protonated. The corresponding hydrogen atom establishes an intramolecular hydrogen bond to the

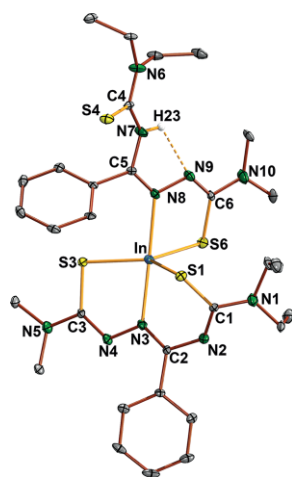


Figure 2. Ellipsoid representation of the molecular structure of $[\text{In}(\text{L}^{\text{H}})(\text{HL}^{\text{H}})]$. Ellipsoids are drawn at the 50 % probability level. Hydrogen atoms (except H23) are omitted for clarity.

nitrogen atom N9 (Figure 2). Such a coordination mode results in the formation of a distorted trigonal-bipyramidal coordination sphere for the indium ion, where the trigonal basal plane is formed by the three sulfur atoms and the apical positions are occupied by the nitrogen donors. Selected bond lengths and angles are summarized in Table 1.

Table 1. Selected bond lengths /Å and angles /° in the indium(III) complexes under study. The values for $(\text{HNEt}_3)[\text{In}(\text{L}^{\text{CF}_3})_2]$ are taken from two crystallographically independent species.

	$[\text{In}(\text{L}^{\text{H}})(\text{HL}^{\text{H}})]$	$[\text{In}(\text{L}^{\text{F}})(\text{HL}^{\text{F}})]$	$(\text{Et}_3\text{NH})[\text{In}(\text{L}^{\text{CF}_3})_2]$
In1–S1	2.4855(6)	2.4533(7)	2.568(1)/2.603(1)
In1–S3	2.4280(6)	2.4466(8)	2.534(1)/2.552(1)
In1–S4	–	–	2.611(1)/2.569(1)
In1–S6	2.4527(6)	2.4580(7)	2.539(1)/2.526(1)
In1–N3	2.254(2)	2.239(2)	2.295(4)/2.295(4)
In1–N8	2.284(2)	2.331(2)	2.269(4)/2.269(4)
C1–S1	1.784(2)	1.796(3)	1.749(5)/1.751(5)
C1–N2	1.300(3)	1.307(4)	1.361(5)/1.326(6)
N2–C2	1.372(3)	1.364(4)	1.372(6)/1.358(6)
C2–N3	1.307(3)	1.307(4)	1.306(6)/1.300(6)
N3–N4	1.390(3)	1.393(3)	1.405(5)/1.407(5)
N4–C3	1.305(3)	1.306(4)	1.299(6)/1.305(7)
C3–S3	1.770(2)	1.770(3)	1.752(5)/1.755(6)
C4–S4	1.668(2)	1.673(3)	1.746(5)/1.753(5)
C4–N7	1.390(3)	1.396(4)	1.315(6)/1.303(6)
N7–C5	1.374(3)	1.375(4)	1.359(5)/1.379(5)
C5–N8	1.303(3)	1.306(4)	1.296(6)/1.300(6)
N8–N9	1.393(3)	1.394(3)	1.412(5)/1.415(4)
N9–C6	1.312(3)	1.311(4)	1.319(6)/1.303(6)
C6–S6	1.759(2)	1.751(3)	1.734(5)/1.760(5)
S1–In–S3	135.15(2)	125.42(3)	154.53(5)/153.07(5)
S3–In–S6	119.10(2)	126.98(3)	101.27(5)/101.34(5)
S1–In–S4	–	–	83.97(4)/83.26(4)
S6–In–S1	105.50(2)	106.34(3)	93.32(4)/93.46(4)
S1–In–N3	85.20(5)	86.92(6)	81.9(1)/80.3(1)
S6–In–N3	104.05(5)	94.46(6)	100.8(1)/102.6(1)
S3–In–N3	80.06(5)	78.95(6)	75.0(1)/74.7(1)
N3–In–N8	176.39(7)	158.26(8)	173.7(2)/174.2(2)

The C–N bond lengths inside the chelate rings of the $\{\text{HL}^{\text{H}}\}^-$ and $\{\text{L}^{\text{H}}\}^{2-}$ ligands are equal to a large extent. This proves the presence of extended π -systems, which also include the exocyclic C1–N1, C3–N5 and C6–N10 bonds. Similar bonding situations have been found in rhenium, technetium and gold complexes with such ligands.^[25,27,29] Also the C–S bonds in the chelate rings of $[\text{In}(\text{L}^{\text{H}})(\text{HL}^{\text{H}})]$ are widened to values between 1.759 and 1.786 Å, while the corresponding C–S bond of the non-coordinating sulfur atom is clearly shorter.

Although the coordination chemistry of the p-block element indium is dominated by six-coordinate complexes, compounds with the coordination number 5 are not rare, and there exists particularly a number of complexes with three trigonal sulfur and two axial nitrogen atoms,^[15,30–36] a constellation, which is also observed in $[\text{In}(\text{L}^{\text{H}})(\text{HL}^{\text{H}})]$.

The basal plane of the trigonal bipyramid is distorted with S–In–S angles between 105.50(2) and 135.15(2)°, while the N3–In–N8 angles of 176.39(7)° come close to the ideal linear arrangement of the two nitrogen donors. The In–S bond lengths are between 2.4280(6) and 2.4855(6) Å, while the In–N distances are around 2.2 Å. These values are in the characteristic range for In thiosemicarbazone complexes.^[37] All C–N bond lengths

are in the range between 1.300 and 1.393 Å irrespective to the fact if they are included into chelate rings or not. This suggests that the electron density shows a high degree of delocalization and the negative charge(s) of the ligand(s) is (are) widely distributed on the whole π -system. The respective bond orders are between double and single bonds.

The molecular structure of the uncoordinated compound $\text{H}_2\text{L}^{\text{H}}$ has also been determined by X-ray diffraction and discussed in a previous report.^[25] In the solid state, the molecule is found in its "thiosemicarbazide" tautomeric form, in which the two nitrogen atoms of the N–N group are protonated and the PhC–N bond of the benzoylthiourea moiety has predominantly double bond character. Upon coordination and formation of the dianion, the two negative charges are delocalized. The C=S bonds are slightly elongated with a consequent increase of the thiolate character of the sulfur donor atoms. In the monoanionic ligand of $[\text{In}(\text{L}^{\text{H}})(\text{HL}^{\text{H}})]$ the non-coordinating C4–S4 bond is shortened in comparison to $\text{H}_2\text{L}^{\text{H}}$. The thiosemicarbazide moieties of both ligands are essentially planar, while the thiourea C=S group of the dianionic ligand deviates strongly from the planarity in order to accommodate the geometrical demands of the metal center. The sulfur atom S4 of the non-coordinating thiocarbonyl group shows a Z arrangement to the coordinating sulfur atom and the backbone of the related molecule is almost planar with slightly deviations for the sulfur atoms. The hydrogen atom on N7 points towards N9 with formation of a hydrogen bond that establishes a planar five-membered ring (see Figure 2). The H23...N9 distance is 2.09 Å and the bonding angle between donor and acceptor is 114.07°. The formation of this relatively strong intramolecular hydrogen bond in the solid state may contribute to the stabilization of the pentacoordinate isomer of the complex. Our attempts to enforce a second deprotonation of this ligand and the formation of an octahedral indium(III) complex by the addition of a base such as NEt_3 to solutions of the pentacoordinate compound in organic solvents failed.

A similar procedure as described for the synthesis of $[\text{In}(\text{L}^{\text{H}})(\text{HL}^{\text{H}})]$ was applied for the reaction of InCl_3 with the *para*-fluorinated thiosemicarbazone $\text{H}_2\text{L}^{\text{F}}$ and led to the formation of a yellow solid, which precipitated from a solution of the reactants in MeOH.

The results of elemental analysis, mass spectrometric and IR spectroscopic studies suggest a composition of the product, which is similar to that with $\text{H}_2\text{L}^{\text{H}}$, having two differently bonded thiosemicarbazones in the coordination sphere of the indium(III) ion: $[\text{In}(\text{L}^{\text{F}})(\text{HL}^{\text{F}})]$. Although the compound is sparingly soluble in common solvents and slowly decomposes in solution, ^1H and ^{19}F NMR spectra of reasonable quality could be recorded and allow conclusions concerning the structure of the compound. The ^1H NMR spectrum of the product is very similar to that of $[\text{In}(\text{L}^{\text{H}})(\text{HL}^{\text{H}})]$ with the signals of the aromatic protons being distributed over a large range. Couplings with the ^{19}F nucleus of the fluorine substituent allow the assignment of signals belonging to two non-equivalent coordinating thiosemicarbazones. Also the ^{19}F NMR presents two multiplets with an integration ratio of 1:1, corresponding to the two differently coordinated ligands.

The conclusions drawn from the spectroscopic studies are confirmed by X-ray diffraction. The solid-state structure of $[\text{In}(\text{L}^{\text{F}})(\text{HL}^{\text{F}})]$ does not differ significantly from that of $[\text{In}(\text{L}^{\text{H}})(\text{HL}^{\text{H}})]$. The indium atom is pentacoordinate with a trigonal bipyramidal geometry, in which the edges of the basal plane are occupied by the sulfur atoms and the apical positions by the nitrogen atoms. Since the molecular structure of $[\text{In}(\text{L}^{\text{F}})(\text{HL}^{\text{F}})]$ is virtually identical with that of the non-fluorinated complex, there is no extra figure given here. But Table 1 contains selected bond lengths and angles of this compound and an ellipsoid representation is depicted in the Supporting Information.

The fluorine substitution seems to induce a sensibly stronger distortion from the ideal geometry. While the N3–In–N8 axis is almost linear in $[\text{In}(\text{L}^{\text{H}})(\text{HL}^{\text{H}})]$, this angle is reduced to a value of 158.26(8)° in the complex with the fluorinated ligand. However, no remarkable effects on the bond lengths could be identified. Similar findings have been reported for oxidorhenium(V) complexes with fluorinated thiosemicarbazones.^[27] The characteristic intramolecular hydrogen bond observed in $[\text{In}(\text{L}^{\text{H}})(\text{HL}^{\text{H}})]$ is also found in $[\text{In}(\text{L}^{\text{F}})(\text{HL}^{\text{F}})]$. Here, the H23...N9 distance is 2.044 Å and the angle between donor and acceptor is 116.99°.

An unexpected result was obtained from the reaction of InCl_3 with the trifluoromethyl-substituted ligand $\text{H}_2\text{L}^{\text{CF}_3}$. Applying the same reaction conditions as for the reactions with $\text{H}_2\text{L}^{\text{H}}$ and $\text{H}_2\text{L}^{\text{F}}$, no precipitation of a solid was observed, but a clear, deep yellow solution was formed. A considerable decomposition of the dissolved product was observed at room temperature according to the recorded NMR spectra. At temperatures between –20 and 0 °C, however, the product is stable in solution. After concentration in an ice-bath and storing at –20 °C for three days, bright yellow crystals precipitated. They were dried under vacuum and re-dissolved in cold CDCl_3 for spectroscopic studies.

At first glance, the ^1H NMR spectrum of the product does not present significantly different features from the previously described complexes. A broad NH signal, which corresponds to a protonated thiosemicarbazone in the ligand is found at 9.35 ppm. Moreover, it is possible to distinguish two coordinated thiosemicarbazone ligands with different ^1H chemical shifts. It is, hence, strongly indicated that the structure of the complex is – at least in solution – the same as those observed for the related products with $\text{H}_2\text{L}^{\text{H}}$ and $\text{H}_2\text{L}^{\text{F}}$. The ^{19}F NMR spectrum of the product confirms this hypothesis: it contains two signals with a 1:1 ratio corresponding to two differently coordinating fluorinated ligands (see Supporting Information). Despite these striking similarities, some extraneous signals are observed in the aliphatic region: a quadruplet at 2.81 ppm and a triplet at 1.22 ppm, indicating the presence of NEt_3 or HNEt_3^+ cations. The ESI+ mass spectrum confirms this assumption and a peak at $m/z = 102.1283$ can unequivocally be assigned to HNEt_3^+ . In addition, also the presence of $[\text{In}(\text{L}^{\text{CF}_3})(\text{HL}^{\text{CF}_3})]$ is clearly detected by an intense peak at $m/z = 923.1428$ ($[\text{M} + \text{H}]^+$). This is in accord with the detection of corresponding molecular ion peaks $[\text{M} + \text{H}]^+$ in the spectra of $[\text{In}(\text{L}^{\text{H}})(\text{HL}^{\text{H}})]$ and $[\text{In}(\text{L}^{\text{F}})(\text{HL}^{\text{F}})]$ at $m/z = 787.1677$ and 823.1390, respectively. However, the negative mode ESI mass spectrum of the indium

complex with the CF₃-substituted thiosemicarbazone shows a signal at *m/z* = 921.1252, which perfectly fits with an [In(L^{CF3})₂]⁻ anion.

The formation of a complex anion with two {L^{CF3}}²⁻ ligands is finally confirmed by single-crystal X-ray diffraction. (HNEt₃)[In(L^{CF3})₂] crystallizes in the triclinic space group *P* $\bar{1}$ with each two complex anions and triethylammonium cations in the asymmetric unit. The two tridentate thiosemicarbazonato ligands coordinate facially and form a strongly distorted octahedral coordination sphere around the indium ion, in which the four sulfur atoms are found in one plane. An ellipsoid representation of the complex anion is given in Figure 3a. Main distortions are due to the angular restrictions induced by the facial arrangement of the chelating ligands. The formation of each two five- and six-membered chelate rings results in angles between adjacent donor atoms in the range from 74.7(1) to 102.6(1)°. It is remarkable that the In–S bond lengths increase upon the formation of the octahedral complex from values between 2.428(1) and 2.485(1) Å in [In(L^H)(HL^H)] and [In(L^F)(HL^F)] to the range 2.526(1) – 2.603(1) in [In(L^{CF3})₂]⁻.

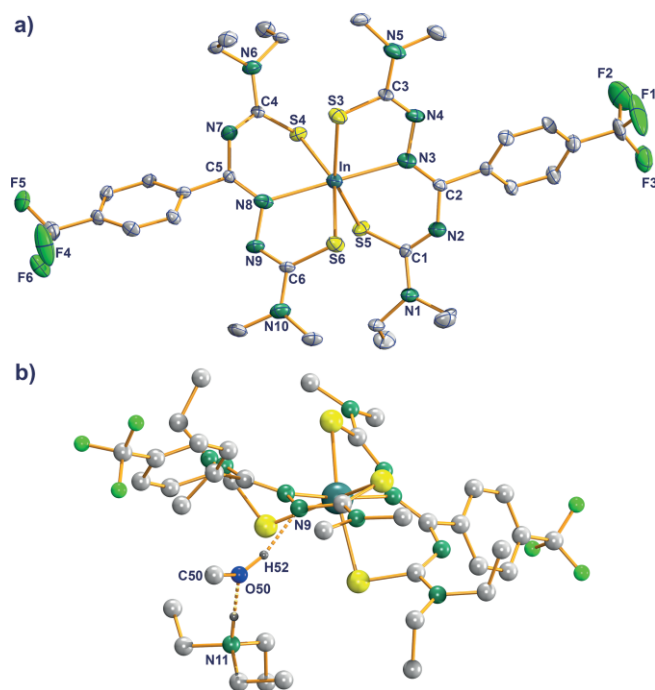


Figure 3. (a) Ellipsoid representation of the complex anion of (HNEt₃)[In(L^{CF3})₂]. Ellipsoids are drawn at the 50 % probability level. Hydrogen atoms are omitted for clarity. (b) Hydrogen bonds established between solvent methanol and the HNEt₃⁺ cation and the [In(L^{CF3})₂]⁻ anion.

There are no appreciable direct intermolecular interactions between the [In(L^{CF3})₂]⁻ anions and the (HNEt₃)⁺ counterions in the solid-state structure of the complex. But the co-crystallized methanol establishes hydrogen bonds between the two ions as is shown in Figure 3b. Hence, the trifluoromethylation of the thiosemicarbazone can only be regarded as one of the reasons for the preference of a six-coordinate indium(III) complex with this particular ligand.

It has been previously observed that the fluorination of the phenyl group of such thiosemicarbazones exerts some influence on the structure of the compound, e.g. the preference of the “thiosemicarbazone” tautomer over the “thiosemicarbazide” form upon CF₃ substitution,^[26] but only a minor influence on the coordination behavior of fluorinated thiosemicarbazones in related rhenium(V), technetium(V) and gold(III) complexes was observed.^[27,2]

In order to get a deeper insight into the observed equilibrium between [In(L^{CF3})(HL^{CF3})] and [In(L^{CF3})₂]⁻, we performed some DFT calculations on the B3LYP level. We first optimized the systems “NEt₃ + [In(L)(HL)]” vs. “(HNEt₃)⁺ + [In(L)₂]⁻” for H₂L = H₂L^H, H₂L^F and H₂L^{CF3} in the gas-phase. In the gas-phase, we found an energetic preference for the neutral species NEt₃ and [In(L)(HL)] compared to the (HNEt₃)[In(L)₂] salts for all three thiosemicarbazones. We then recalculated these pre-optimized structures for both the associated and the fully separated pairs in methanol solution. We found an energetic preference in the free energy for the non-interacting species both for the triethylammonium salts (between 28 and 42 kJ/mol) and the neutral species (between 53 and 57 kJ/mol). Therefore, we assume that mainly non-aggregated compounds are present in solution. In the separated, solvated molecules, we found a preference in the free energy for the pentacoordinate, neutral species in all cases (12 to 27 kJ/mol depending on the substitution). This is consistent with the experimental observation of pentacoordinate species in solution and the observed deprotonation of (HNEt₃)⁺ by [In(L^{CF3})₂]⁻ with formation of NEt₃ and [In(HL^{CF3})(L^{CF3})] upon dissolution. As the salt (HNEt₃)⁺[In(L^{CF3})₂]⁻ was observed in the solid state, where the molecules are definitely closer and undoubtedly more likely to interact with each other, we reinvestigated the free energy differences between the salt and the neutral species in the solvated associated pairs of molecules. For the CF₃-substituted complexes, a preference in the free energy of ca. 4.7 kJ/mol for the salt structure was found, while for H₂L^H both structures are isoenergetic and for H₂L^F a slight preference of only 1.9 kJ/mol for the neutral species were found. The relevant free energies are shown in Table 2.

Table 2. Free energies ΔG at 298.15 K after quasi-harmonic Grimme correction (free-rotor treatment of frequencies below 500 cm⁻¹ with harmonic approximation of the remaining frequencies) calculated for the NEt₃ + [In(L)(HL)] vs. (HNEt₃)⁺ + [In(L)₂]⁻ equilibrium in the MeOH solution for both associated and fully separated moieties. The energies of the most stable side of the equilibrium are bold.

	“NEt ₃ + [In(L)(HL)]”		“(HNEt ₃) ⁺ + [In(L) ₂] ⁻ ”		$\Delta(\Delta G)/\text{kJ mol}^{-1}$	
	associated	separated	associated	separated	associated	separated
H ₂ L ^H $\Delta G/\text{Hartree}$	-3602.924861	-3602.94652	-3602.924862	-3602.93629	0	26.9
H ₂ L ^F $\Delta G/\text{Hartree}$	-3801.410308	-3801.43049	-3801.409594	-3801.42559	1.9	12.8
H ₂ L ^{CF3} $\Delta G/\text{Hartree}$	-4276.995318	-4277.01639	-4276.997116	-4277.0077	4.7	22.8

Overall, the aggregation in the solid state is the most probable driving force in the formation of the salt, albeit the energetic differences between neutral and charged species upon aggregation are small in solution, the complexes derived from $\text{H}_2\text{L}^{\text{CF}_3}$ appear to be the most favorable to form $[\text{In}(\text{L})_2]^-$. The observed hydrogen bonding might further stabilize the solid-state structure of $(\text{HNEt}_3)^+[\text{In}(\text{L}^{\text{CF}_3})_2]^-$.

As we only prepared three derivatives of the present complexes, we additionally performed calculations on the hypothetical complex pairs of $\text{H}_2\text{L}^{\text{Cl}}$, $\text{H}_2\text{L}^{\text{Br}}$, $\text{H}_2\text{L}^{\text{I}}$ and $\text{H}_2\text{L}^{\text{CH}_3}$. We calculated their theoretical thermodynamic K_{eq} at $T = 298.15 \text{ K}$ [$\ln(K_{\text{eq}}) = -\Delta G/(RT)$; $R = 0.008314 \text{ kJ mol}^{-1} \text{ K}^{-1}$] to establish a Hammett relation between the acidities of the complexes and the electronic properties of the substituents. The different theoretical acidities of the pentacoordinate In^{III} complexes (in the form of the theoretical K_{eq} in the described equilibrium) of the fluorinated ligands do not correlate well with the electronic Hammett parameters ($\rho = 1.7$, $R^2 = 0.12$). This suggests only a minor electronic influence of the CF_3 and F substituents on the acidities, which finally also agrees with the similar chemical shifts of the related protons in the ^1H NMR spectra. However, for the complexes of the hypothetical heavier halogen and methyl-substituted ligands an excellent correlation between the Hammett parameters of the substituents with the acidities is found, when the anomalous fluorine-containing derivatives are neglected ($\rho = 4.5$, $R^2 = 0.95$). The respective ρ value suggests a reasonably strong electronic influence of the *para*-substituent. The correlation holds true for both, the σ_{p} and the corrected $\sigma_{\text{p}}^+/\sigma_{\text{p}}^-$ Hammett parameters. Further information on the calculations is provided in the Supporting Information.

The re-conversion of the octahedral complex into the more stable five-coordinate compound upon dissolution can be avoided, when the anion is precipitated with a non-protic counterion such as NBu_4^+ . In this case, the octahedral structure is maintained in solution, which can be verified by the appearance of only one ^{19}F NMR signal for the dissolved tetrabutylammonium salt. A corresponding NMR experiment on a mixture of $(\text{NBu}_4)[\text{In}(\text{L}^{\text{CF}_3})_2]$ and $(\text{HNEt}_3)[\text{In}(\text{L}^{\text{CF}_3})_2]$ confirms this finding. Both complexes form the octahedral isomer in the solid state. After dissolution in CDCl_3 , only the fraction, which corresponds to the used amount of HNEt_3^+ salt shows isomerization to the five-coordinate complex by the appearance of two ^{19}F NMR signals (see Supporting Information). This confirms the triethylammonium ion as proton source for the observed partial protonation of the $\{\text{L}^{\text{CF}_3}\}_2^-$ ligand.

Conclusions

Reactions of InCl_3 with three potentially *S,N,S*-tridentate thiosemicarbazones derived from differently substituted *N,N*-diethyl-*N'*-benzoylthioureas gave pentacoordinate, neutral bis-chelates of the composition $[\text{In}(\text{L})(\text{HL})]$ in solution. A tridentate coordination of one and a bidentate *S,N*-coordination of the second ligand was deduced from the IR, $^1\text{H}/^{19}\text{F}$ NMR and ESI-MS spectra of the products. DFT calculations confirm the high stability of the five-coordinate compounds with one non-coordinated thiocarbonyl group. The formation of an anionic, six-

coordinate indium complex was only observed for the trifluoromethyl-substituted ligand. In the solid state, an $[\text{In}(\text{L}^{\text{CF}_3})_2]^-$ complex with a distorted octahedrally coordinated In^{III} ion is formed. Upon dissolution, the HNEt_3^+ salt of this complex reforms the more stable, neutral $[\text{In}(\text{L}^{\text{CF}_3})(\text{HL}^{\text{CF}_3})]$ complex under deprotonation of the triethylammonium cation.

Experimental Section

All chemicals and reagents were purchased from commercial sources and used without further purification. The thiosemicarbazone ligands were synthesized according to the procedure described in the literature.^[26]

NMR spectra were recorded with a JEOL 400 MHz multinuclear spectrometer. Positive- and negative-mode ESI mass spectra were measured with an Agilent 6210 ESI-TOF (Agilent Technology) mass spectrometer. Elemental analysis of carbon, hydrogen, nitrogen and sulfur were performed using a Heraeus elemental analyzer. For the IR spectra a Nicolet iS10 FT-IR spectrometer was used.

The intensities for the X-ray determinations were collected on a Bruker D8 Venture instrument with Mo-K_α radiation. Structure solution and refinement were performed with the SHELX program packages.^[38,39] Hydrogen atoms were placed at calculated positions and treated with the "riding model" option of SHELXL, except those of the NH groups of the thiosemicarbazones. Their positions of were taken from the Fourier map. The representation of molecular structures was done using the program DIAMOND (vers. 4.5.1).^[40] Additional information on the structure determinations is contained in the Supporting Information.

CCDC 1966320 {for $[\text{In}(\text{HL}^{\text{H}})(\text{L}^{\text{H}})] \cdot 1.5\text{benzene}$ }, 1966321 {for $[\text{In}(\text{HL}^{\text{F}})(\text{L}^{\text{F}})]$ }, 1966322 {for $(\text{HNEt}_3)[\text{In}(\text{L}^{\text{CF}_3})_2] \cdot \text{MeOH}$ } contain the supplementary crystallographic data for this paper. These data can be obtained free of charge from The Cambridge Crystallographic Data Centre.

DFT calculations were performed on the high-performance computing systems of the Freie Universität Berlin ZEDAT (Curta) using the program packages GAUSSIAN 09 and GAUSSIAN 16.^[41,42] The gas phase geometry optimizations were performed using coordinates derived from the X-ray crystal structures or have been modelled with the use of crystal structure fragments using GAUSSVIEW.^[43] The calculations in solutions were performed on structures, which were previously optimized in the gas-phase. The polarizable continuum model (PCM) with the integral equation formalism variant (IEFPCM) was used to implicitly simulate the solvent methanol. The calculations were performed with the hybrid density functional B3LYP.^[44–46] The Stuttgart double- ζ relativistic large core (RLC) basis set with the respective effective core potential (ECP) was applied to In .^[47,48] For I, the 6-311G* basis set was applied.^[49] The 6-31G* basis set was applied for all other atoms,^[50–53] except for H, for which the smaller 6-31G was employed.^[54] The Stuttgart RLC, 6-31G* and 6-31G basis sets as well as the RLC-ECP were obtained from the EMSL database.^[55] The convergence of the structures was verified by frequency calculations. No negative frequencies were obtained confirming the optimized geometries as energetic minima. The entropic contribution to the free energy was corrected for low-energy modes using the quasi-harmonic approximation of Grimme^[56] as implemented in the freely accessible python code *GoodVibes* of Funes-Ardoiz and Paton with a cut-off at 500 cm^{-1} .^[57] The σ_{p} and the corrected $\sigma_{\text{p}}^+/\sigma_{\text{p}}^-$ Hammett parameters were taken from a tabulated review article.^[58]

[In(L^H)(HL^H)]: InCl₃ (22 mg, 0.1 mmol) was dissolved in 3 mL of MeOH and cooled to 0 °C. Subsequently, H₂L^H (69 mg, 0.2 mmol) and NEt₃ (101 mg, 1.0 mmol) were added. Upon addition of the base, the suspension turned into a clear yellow solution, which was stirred until the formation of a yellow precipitate. The precipitate was filtered off and dried under vacuum. Single crystals suitable for X-ray structure determination were grown from a concentrated benzene solution at 6 °C. Yield: 98 %. Elemental analysis: Calculated for C₃₀H₄₅N₁₀S₄In: C 45.7, H 17.2, N 17.8, S 16.3 %; found C, 44.1; H 5.3, N 17.2, S 15.5 %. IR (ν in cm⁻¹): $\tilde{\nu}$ = 3238 w (NH), 2968 m, 2928 m, 2869 m, 1585 w, 1561 w, 1493 s (C=N), 1455 m, 1414 m, 1374 m, 1351 s, 1305 m, 1253 s, 1212 w, 1177 w, 1128 s, 1094 s, 1071 s, 1027 m, 1000 m, 906 s, 854 m, 772 s, 725 s, 694 s, 646 m. ¹H NMR (CDCl₃, ppm): δ = 9.26 (s, 1H, NH), 7.82 (m, 2H, Ph), 7.53–7.40 (m, 5H, Ph), 7.28–7.22 (s, 3H, Ph), 4.04–3.52 (broad, 8H, N-CH₂), 6.36 (broad m, 1H, N-CH₂), 3.19 (s, 6H, N-CH₃), 2.93 (s, 6H, N-CH₃), 1.22 (m, 12H, CH₂-CH₃). MS ESI+ (*m/z*): 787.1677 (calc. 787.1683) [M + H]⁺, 809.1480 (calc. 809.7929) [M + Na]⁺, 825.1219 (calc. 825.1242) [M + K]⁺, 714.0778 (calc. 714.0792) [M - NEt₃]⁺, 234.1062 (calc. 234.1065) [C₁₂H₁₆N₃S]⁺ (imidium ion of the benzoylthiourea).

[In(L^F)(HL^F)]: InCl₃ (22 mg, 0.1 mmol) was dissolved in 3 mL of MeOH and cooled to 0 °C. Subsequently, H₂L^F (71 mg, 0.2 mmol) and NEt₃ (101 mg, 1.0 mmol) were added whilst stirring. Upon addition of the base, the suspension turned into a clear yellow solution and a yellow solid starts to precipitate after a few seconds. The precipitate was filtered off and dried under vacuum. Single crystals suitable for X-ray structure determination were grown by slow diffusion of pentane in a CH₂Cl₂ solution at -20 °C over a period of 2 weeks. Yield: 78 %. Elemental analysis: Calculated for C₃₀H₄₁F₂InN₁₀S₄: C 43.8, H 5.0, N 17.0, S 15.6 %; found C 42.5, H 5.1, N 17.0, S 15.5 %. IR (ν in cm⁻¹): $\tilde{\nu}$ = 3225 w (NH), 2940 w, 1597 w, 1560 w, 1525 m, 1495 s (C=N), 1458 m, 1451 m, 1431 m, 1412 m, 1353 s, 1311 m, 1264 m, 1229 m, 1219 m, 1182 w, 1141 m, 1087 m, 1077 m, 1053 w, 1027 w, 1000 w, 1010 w, 939 w, 909 m, 898 w, 865 m, 856 m, 847 m, 831 m, 816 w, 803 w, 789 w, 766 w, 747 w, 732 w, 715 w, 689 m, 649 m, 639 m, 626 m, 613 m. ¹H NMR (CDCl₃, ppm): δ = 9.30 (s, 1H, NH), 7.88 (m, 2H, Ph), 7.46 (m, 2H, Ph), 7.12 (m, 2H, Ph), 6.94 (m, 2H, Ph), 3.87 (broad, 4H, N-CH₂), 3.66 (broad 4H, N-CH₂), 3.19 (s, 6H, N-CH₃), 2.96 (s, 6H, N-CH₃), 1.33–1.17 (broad, 12H, CH₂-CH₃). ¹⁹F NMR (CDCl₃, ppm): δ = -108.74 (m, 1F), -111.94 (m, 1F). MS ESI+ (*m/z*): 823.1390 (calc. 823.1484) [M + H]⁺.

(HNEt₃)[In(L^{CF3})₂]: InCl₃ (22 mg, 0.1 mmol) was dissolved in 3 mL of MeOH and cooled to 0 °C. Subsequently, H₂L^{CF3} (81 mg, 0.2 mmol) and NEt₃ (101 mg, 1.0 mmol) were added. The suspension was stirred until a clear yellow solution was obtained. Concentration under vacuum in an ice bath followed by standing at -20 °C for 1–2 days led to the formation of yellow crystals, which were dried under vacuum. Single crystals suitable for X-ray structure determination were grown from MeOH at -20 °C. Yield: 95 %. Elemental analysis: Calculated for C₃₈H₅₈F₆N₁₁S₄In: C 44.5, H 12.5, N 15.0, S 12.5 %; found C 44.6, H 5.5; N 15.1, S 12.6 %. IR (ν in cm⁻¹): $\tilde{\nu}$ = 2977 m, 2930 m, 2602 m, 2496 m, 1476 m, 1444 m, 1397 m, 1354 m, 1321 s, 1243 m, 1215 w, 1164 m, 1122 s, 1099 s, 1067 s, 1035 s, 1016 m, 913 m, 850 s, 806 m, 756 w, 694 w, 604 m. ¹H NMR (CDCl₃, ppm): δ = 9.35 (s, 1H, NH), 7.94 (m, 2H, Ph), 7.68 (m, 2H, Ph), 7.58 (m, 2H, Ph), 7.52 (m, 2H, Ph), 3.94–3.60 (broad m, 7H, N-CH₂), 3.40 (broad m, 1H, N-CH₂), 3.21 (s, 6H, N-CH₃), 2.92 (s, 6H, N-CH₃), 2.81 (q, triethylamine), 1.40–1.07 (overlapped t, CH₂-CH₃ + triethylamine). ¹⁹F NMR (CDCl₃, ppm): δ = -62.60 (s, 3F), -62.64 (s, 3F). MS-ESI+ (*m/z*): 923.1428 (calc. 923.1431) [M + H]⁺, 102.1283 (calc. 102.1283) [Et₃NH]⁺. MS ESI- (*m/z*): 921.1252 (calc. 921.1263) [M]⁻.

Acknowledgments

This work was generously supported by the Graduate School (GK 1582) “Fluorine as a key element” of the Deutsche Forschungsgemeinschaft. We also gratefully acknowledge the assistance of the Core Facility BioSupraMol supported by the DFG and the High-Performance-Computing (HPC) Centre of the Zentralinstitut für Datenverarbeitung (ZEDAT) of the Freie Universität Berlin for computational time and support.

Keywords: Indium · Thiosemicarbazones · Fluorinated ligands · Coordination number · Isomerization

- [1] R. E. Weiner, M. L. Thakur in *Handbook of radiopharmaceuticals – radiochemistry and applications*, Vol. 11 (Eds.: M. J. Welch, C. S. Redvanly), John Wiley & Sons, Inc., Chichester, **2005**, pp. 363–399.
- [2] P. J. Blower, *Dalton Trans.* **2015**, 44, 4819–4844.
- [3] E. W. Price, J. F. Cawtray, G. A. Bailey, C. L. Ferreira, E. Boros, M. J. Adam, C. Orvig, *J. Am. Chem. Soc.* **2012**, 134, 8670–8683.
- [4] V. Kuntic, J. Brboric, Z. Vujic, S. Uskokovic-Markovic, *Asian J. Chem.* **2016**, 28, 235–241.
- [5] J. R. Dilworth, S. I. Pascu in *The Chemistry of Molecular Imaging*, Vol. 7 (Eds.: N. Long, W. T. Wong) John Wiley & Sons, Inc., New Jersey, **2009**, pp. 165–178.
- [6] E. N. Kaya, M. Durmuş, M. Bulut, *J. Organomet. Chem.* **2014**, 774, 94–100.
- [7] S. Tajbakhsh, K. Mohammadi, I. Deilami, K. Zandi, M. Fouladvand, E. Ramjedani, G. Asayesh, *Afr. J. Biotechnol.* **2008**, 7, 3832–3835.
- [8] H. J. Rogers, C. Synge, V. E. Woods, *Antimicrob. Agents Chemother.* **1980**, 18, 63–68.
- [9] S. David, V. Barros, C. Cruz, R. Delgado, *FEMS Microbiol. Lett.* **2005**, 251, 119–124.
- [10] K. Mohammadi, K. H. Thompson, B. O. Patrick, T. Storr, C. Martins, E. Polishchuk, V. G. Yuen, J. H. McNeill, C. Orvig, *J. Inorg. Biochem.* **2005**, 99, 2217–2225.
- [11] M. Asadi, N. Savaripoor, Z. Asadi, M. H. Ghatee, F. Moosavi, R. Yousefi, M. Jamshidi, *Spectrochim. Acta* **2013**, 101, 394–399.
- [12] S. P. Petrosyants, A. B. Ilyukhin, *Russ. J. Inorg. Chem.* **2011**, 56, 2047–2069.
- [13] H. V. Rasika Dias, *Comprehensive coordination chemistry II*, Vol. 3 (Eds.: J. A. McCleverty, T. J. Meyer), Elsevier Science **2003**, pp. 383–450.
- [14] T. J. Wadas, E. H. Wong, G. R. Weisman, C. J. Anderson, *Chem. Rev.* **2010**, 110, 2858–2902.
- [15] J. McB. Harrowfield, C. Pakawatchai, A. H. White, *J. Chem. Soc., Dalton Trans.* **1983**, 1109–1113.
- [16] S. Abram, C. Maichle-Mössmer, U. Abram, *Polyhedron* **1998**, 17, 131–143.
- [17] J. Chan, A. L. Thompson, M. W. Jones, J. M. Peach, *Inorg. Chim. Acta* **2010**, 363, 1140–1149.
- [18] R. L. Arrowsmith, P. A. Waghorn, M. W. Jones, A. Bauman, S. K. Brayshaw, Z. Hu, G. Kociok-Kohn, T. L. Mindt, R. M. Tyrrell, S. W. Botchway, J. R. Dilworth, S. I. Pascu, *Dalton Trans.* **2011**, 40, 6238–6252.
- [19] Y.-X. Tai, Y.-M. Ji, Y.-L. Lu, M.-X. Li, Y.-Y. Wu, Q.-X. Han, *Synth. Met.* **2016**, 219, 109–114.
- [20] A. Molter, F. Mohr, *Dalton Trans.* **2011**, 40, 3754–3758.
- [21] Y.-T. Wang, Y. Fan, M. Zhao, M.-X. Li, Y.-M. Ji, Q.-Y. Han, *Med. Chem. Commun.* **2017**, 8, 2125–2132.
- [22] A. A. Oliveira, G. M. C. Perdigao, L. E. Rodrigues, J. G. da Silva, E. M. Souza-Fagundes, J. A. Takahashi, W. R. Rocha, H. Beraldo, *Dalton Trans.* **2017**, 46, 918–932.
- [23] A. A. Oliveira, G. M. C. Perdigao, J. G. da Silva, E. M. Souza-Fagundes, H. Beraldo, *Polyhedron* **2017**, 135, 72–78.
- [24] A. A. Oliveira, L. L. Franco, R. G. dos Santos, G. M. C. Perdigao, J. G. da Silva, E. M. Souza-Fagundes, H. Beraldo, *New J. Chem.* **2017**, 41, 9041–9050.
- [25] H. H. Nguyen, P. I. da S. Maia, V. M. Defflon, U. Abram, *Inorg. Chem.* **2009**, 48, 25–27.
- [26] F. Salsi, G. B. Portapilla, K. Schutjajew, Z. A. Carneiro, A. Hagenbach, S. de Albuquerque, P. I. da S. Maia, U. Abram, *J. Fluorine Chem.* **2018**, 215, 52–61.

- [27] F. Salsi, G. Bulhões Portapilla, S. Simon, M. Roca Jungfer, A. Hagenbach, S. de Albuquerque, U. Abram, *Inorg. Chem.* **2019**, *58*, 10129–10138.
- [28] C. Duque Lopes, B. Possato, A. P. S. Gaspari, R. J. Oliveira, U. Abram, J. P. A. Almeida, F. dos Reis Rocho, A. Leitão, C. A. Montanari, P. I. S. Maia, J. S. da Silva, S. de Albuquerque, Z. A. Carneiro, *ACS Infect. Dis.* **2019**, *5*, 1698–1707.
- [29] F. Salsi, G. Bulhões Portapilla, K. Schutjajew, M. Roca Jungfer, A. Goulart, A. Hagenbach, S. de Albuquerque, U. Abram, *Eur. J. Inorg. Chem.* **2019**, 4455–4462.
- [30] I. R. Berina, O. G. Matyukhina, A. N. Sobolev, Y. V. Ashaks, A. Bankovskii, V. S. Fundamenskii, **1985**, Cambridge Structural Data base, entry DAT-SOG.
- [31] S. Suh, D. M. Hoffman, *Inorg. Chem.* **1998**, *37*, 5823–5826.
- [32] R. J. Motekaitis, A. E. Martell, S. A. Koch, J. Hwang, D. A. Quarless Jr., M. J. Welch, *Inorg. Chem.* **1998**, *37*, 5902–5911.
- [33] G. G. Briand, B. F. T. Cooper, D. B. S. MacDonald, C. D. Martin, G. Schatte, *Inorg. Chem.* **2006**, *45*, 8423–8429.
- [34] T. A. Annan, R. Kumar, H. E. Mabrouk, D. G. Tuck, R. K. Chadha, *Polyhedron* **1989**, *8*, 865–871.
- [35] R. D. Schluter, G. Krauter, W. S. Rees Jr., *J. Cluster Sci.* **1997**, *8*, 123–154.
- [36] J. Heine, M. Holynska, M. Reuter, B. Haas, S. Chatterjee, M. Koch, K. I. Gries, K. Volz, S. Dehnen, *Cryst. Growth Des.* **2013**, *13*, 1252–1259.
- [37] J. S. Casas, M. S. Garcia-Tasende, J. Sordo, *Coord. Chem. Rev.* **2000**, *209*, 197–261.
- [38] G. M. Sheldrick, *Acta Crystallogr., Sect. A* **2008**, *64*, 112–122.
- [39] G. M. Sheldrick, *Acta Crystallogr., Sect. C* **2015**, *71*, 3–8.
- [40] K. Brandenburg, Diamond-Crystal and Molecular Structure Visualization, Crystal impact GbR, vers. 4.5.1, **2018**, Bonn (Germany).
- [41] M. J. Frisch, G. W. Trucks, H. B. Schlegel, G. E. Scuseria, M. A. Robb, J. R. Cheeseman, G. Scalmani, V. Barone, B. Mennucci, G. A. Petersson, H. Nakatsuji, M. Caricato, X. Li, H. P. Hratchian, A. F. Izmaylov, J. Bloino, G. Zheng, J. L. Sonnenberg, M. Hada, M. Ehara, K. Toyota, R. Fukuda, J. Hasegawa, M. Ishida, T. Nakajima, Y. Honda, O. Kitao, H. Nakai, T. Vreven, J. A. Montgomery Jr., J. E. Peralta, F. Ogliaro, M. Bearpark, J. J. Heyd, E. Brothers, K. N. Kudin, V. N. Staroverov, R. Kobayashi, J. Normand, K. Raghavachari, A. Rendell, J. C. Burant, S. S. Iyengar, J. Tomasi, M. Cossi, N. Rega, J. M. Millam, M. Klene, J. E. Knox, J. B. Cross, V. Bakken, C. Adamo, J. Jaramillo, R. Gomperts, R. E. Stratmann, O. Yazyev, A. J. Austin, R. Cammi, C. Pomelli, J. W. Ochterski, R. L. Martin, K. Morokuma, V. G. Zakrzewski, G. A. Voth, P. Salvador, J. J. Dannenberg, S. Dapprich, A. D. Daniels, Ö. Farkas, J. B. Foresman, J. V. Ortiz, J. Cioslowski, D. J. Fox, *Gaussian 09, Revision B.01*, Gaussian, Inc., Wallingford CT, **2016**.
- [42] M. J. Frisch, G. W. Trucks, H. B. Schlegel, G. E. Scuseria, M. A. Robb, J. R. Cheeseman, G. Scalmani, V. Barone, G. A. Petersson, H. Nakatsuji, X. Li, M. Caricato, A. Marenich, J. Bloino, B. G. Janesko, R. Gomperts, B. Mennucci, H. P. Hratchian, J. V. Ortiz, A. F. Izmaylov, J. L. Sonnenberg, D. Williams-Young, F. Ding, F. Lipparini, F. Egidi, J. Goings, B. Peng, A. Petrone, T. Henderson, D. Ranasinghe, V. G. Zakrzewski, J. Gao, N. Rega, G. Zheng, W. Liang, M. Hada, M. Ehara, K. Toyota, R. Fukuda, J. Hasegawa, M. Ishida, T. Nakajima, Y. Honda, O. Kitao, H. Nakai, T. Vreven, K. Throssell, J. A. Montgomery Jr., J. E. Peralta, F. Ogliaro, M. Bearpark, J. J. Heyd, E. Brothers, K. N. Kudin, V. N. Staroverov, T. Keith, R. Kobayashi, J. Normand, K. Raghavachari, A. Rendell, J. C. Burant, S. S. Iyengar, J. Tomasi, M. Cossi, J. M. Millam, M. Klene, C. Adamo, R. Cammi, J. W. Ochterski, R. L. Martin, K. Morokuma, O. Farkas, J. B. Foresman, D. J. Fox, *Gaussian 09, Revision A.02*, Gaussian, Inc., Wallingford CT, **2016**.
- [43] *GaussView*, Version 6, Roy Dennington, Todd A. Keith, John M. Millam, Semichem Inc., Shawnee Mission, KS, **2016**.
- [44] S. H. Vosko, L. Wilk, M. Nusair, *Can. J. Phys.* **1980**, *58*, 1200–1211.
- [45] A. D. Becke, *J. Chem. Phys.* **1993**, *98*, 5648–5652.
- [46] C. Lee, W. Yang, R. G. Parr, *Phys. Rev. B* **1988**, *37*, 785–789.
- [47] A. Bergner, M. Dolg, W. Küchle, H. Stoll, H. Preuß, *Mol. Phys.* **1993**, *80*, 1431–1441.
- [48] T. Leininger, A. Berning, A. Nicklass, H. Stoll, H.-J. Werner, H.-J. Flad, *Chem. Phys.* **1997**, *217*, 19–27.
- [49] M. N. Glukhovtsev, A. Pross, M. P. McGrath, L. Radom, *J. Chem. Phys.* **1995**, *103*, 1878–1885.
- [50] M. M. Francl, W. J. Pietro, W. J. Hehre, J. S. Binkley, M. S. Gordon, D. J. DeFrees, J. A. Pople, *J. Chem. Phys.* **1982**, *77*, 3654–3665.
- [51] M. S. Gordon, J. S. Binkley, J. A. Pople, W. J. Pietro, W. J. Hehre, *J. Am. Chem. Soc.* **1982**, *104*, 2797–2803.
- [52] P. C. Hariharan, J. A. Pople, *Theor. Chim. Acta* **1973**, *28*, 213–222.
- [53] W. J. Hehre, R. Ditchfield, J. A. Pople, *J. Chem. Phys.* **1972**, *56*, 2257–2261.
- [54] R. Ditchfield, W. J. Hehre, J. A. Pople, *J. Chem. Phys.* **1971**, *54*, 724–728.
- [55] K. L. Schuchardt, B. T. Didier, T. Elsethagen, L. Sun, V. Gurumoorathi, J. Chase, J. Li, T. L. Windus, *J. Chem. Inf. Model.* **2007**, *47*, 1045–1052.
- [56] S. Grimme, *Chem. Eur. J.* **2012**, *18*, 9955–9964.
- [57] R. Paton, I. Funes-Ardoiz; GoodVibes v.2.0.2; <https://zenodo.org/badge/latestdoi/16266/bobbypaton/GoodVibes>.
- [58] C. Hansch, A. Leo, R. W. Taft, *Chem. Rev.* **1991**, *91*, 165–195.

Received: December 25, 2019